

Gaussian Beam Steering on a Target Plane via High Speed Orthogonal Mirror-mounted Galvanometers

A Senior Project

presented to

the Faculty of the Physics Department

California Polytechnic State University, San Luis Obispo

In Partial Fulfillment

of the Requirements for the Degree

Bachelor of Science

by

Keith Gresiak

June, 2012

© 2012 Keith Gresiak

Abstract

Gaussian beam steering is an important element in many industrial and scientific applications such as medical imaging, laser display, holography, laser cutting, and laser welding. In this investigation the frequency response, angle per volt, and maximum angle for a Nutfield QuantumDrive-1500 model mirror mounted galvanometer and servo system was measured. This system makes use of two orthogonal mirrors to control the x and y axes of the beam on a target plane. The bandwidth of the ensemble was found to be 250 Hz, while the maximum scanning range was measured to be 22.7 degrees in both the x and y directions. This scanning range was found to differ from the manufacturer's specification of 20.0 degrees by only 13.4%. The angle per volt was calculated at 4.55 degree per volt, which agreed favorably to the manufacturer's specifications of 4.00 degrees per volt, a difference of 13.8%. To test the system's functionality as a laser display a circular pattern was used. Because of a 62.48 loops per second data rate, the system behaved quite poorly as a laser display at frequencies upwards of 50 Hz. Therefore, necessary upgrades are needed before this system could be used as a laser display for open house.

Introduction

The development of the galvanometer was one of the biggest contributions to modern analog ammeters and laser beam steering. There are several different types of galvanometers, but the most common and traditional one is the moving coil Weston galvanometer. This type of galvanometer is the most practical for current measuring applications because it is fairly robust using a restoring spring to counter the moving coil. It is not the most accurate galvanometer, however, but it was simple to build and allowed for the possibility of measuring currents.

A drawback of the Weston galvanometer is its response to the earth's magnetic field. As a result, more developments to the galvanometer were made. The "astatic galvanometer," as seen in Figure 1, uses two needles of opposing polarity to effectively cancel the earth's magnetic field and any other external field. This galvanometer cannot be calibrated from first principles and therefore could not be used to quantitatively measure current.

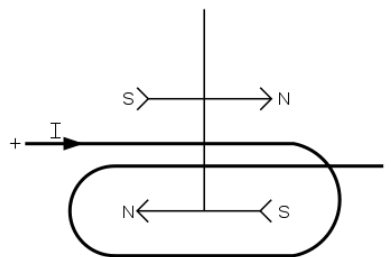


Figure 1. An astatic galvanometer with two opposing poles cancelling the magnetic field due to the earth.

A more modern approach is to attach a mirror to the galvanometer and use a reflected beam of light as the needle. The advantage is a massless and much longer needle. This makes the

system more sensitive and able to resolve smaller amounts of current. With a mirror attached, the ensemble as a whole becomes much more versatile than an ammeter. It becomes a current or voltage controlled rotating mirror mount that has many uses in science and industry.

With the development of the laser, the galvanometer became the standard for steady and fast beam steering. It is now employed in almost all areas where precise beam placement is needed. In industry the galvanometer is used to control laser marking and etching along with cutting. In the semiconductor industry most silicon wafers and chips are cut with a galvanometer-steered laser.

Not only are galvanometers precise, but they also capable of sweeping across target regions in a very quick and controlled fashion. This is useful for barcode scanning and for laser light shows where the beam can be swept faster than the eye can detect. This allows for full images to be displayed using only a single beam.

Perhaps more importantly is the fact that galvanometers have been pivotal in cutting edge research such as optical tweezing and quantum computing, two fields which have very widespread implications. Galvanometers are monumental in the optical tweezing process because it makes for very steady and accurate placement of the tweezers [1]. Optical tweezing is a fairly recent development that allows for researchers in the field of biology and colloidal science to manipulate objects on the micron and submicron scales. This is instrumental in DNA and gene manipulation as scientists attach them to polystyrene beads controlled by galvanometer powered tweezers [2].

Recently researchers out of the Heinrich-Heine University in Dusseldorf, Germany have been studying making multiple optical tweezers traps by coupling the galvanometer controlled laser beam with a spatial light modulator [1]. The spatial light modulator splits the beam up into an array of traps which are then moved smoothly and quickly by the galvanometers. This is a pretty stark improvement over other methods using acousto-optic modulators, where the modulators could not produce as complex a trapping arrangement and also had larger deviations in intensity.

Another important area of galvanometer usage in research is in quantum computing [3]. Here the galvanometer's usage is twofold—to control the optical tweezers or as a means of reading flux qubits. Its usage in optical tweezing is important to trap entangled states or qubits which act as binary bits of data, but it is also used in its more traditional, original form as an amplifier to transform the input signal into a magnetic flux for qubit readout. As modulated microwaves, which are of comparable energy to the energy gap between basis states, are applied, the qubits begin to interact with the field and become entangled. When the qubits spin flip they release small flux qubits which can be measured with very sensitive galvanometers. Scientists out of the University of Wisconsin, Madison have only recently begun to implement microwave amplifying galvanometers instead of the more common superconducting quantum interference device (SQUID) amplifiers used in superconducting quantum circuits in hopes of better responsivity, bandwidth, and ultimately efficient quantum computing, therefore making the galvanometer an important device to study [3].

Theory

In a Weston galvanometer, as seen in Figure 2, there is a rotating knob with a needle fixed to it. Around this rotating mount is a coil of wires and a magnet. When a current from an external circuit or load is fed through the coils the interplay between the magnetic field from the

magnet and from the coils forms a torque on the knob causing the needle to turn. This torque is opposed by the restoring force from a spring also mounted on the knob. When the torque, which is proportional to the current flowing in the coils, is matched by the force of the spring the needle ceases to move and the current can be measured. The relationship between the current, resulting magnetic field, and applied torque is complicated, but as we will see, can be solved for analytically, and therefore, the amount of movement in the needle, or in modern applications a mirror, can be controlled by applying a signal to the coils.

The starting point of this analysis is Biot-Savart's Law which gives a relation for the magnetic field at a test point in terms of a current density, a point within that current density, and the distance from that point to the test point. When looking at an infinitesimal section of current density, the differential contribution to the magnetic field can be expressed as,

$$d\vec{B} = \frac{\mu_0 \vec{J}(\vec{r}') \times \hat{r}}{4\pi r^2} d\tau', \quad (1)$$

where $d\vec{B}$ is the infinitesimal magnetic field, $\vec{J}(\vec{r}')$ is the current density, r is the distance from the section of current density to the test point (which comes from $\vec{r} = \vec{r} - \vec{r}'$), and $d\tau'$ is the volume element of the current [4]. Integrating over the entire current flow will then give us the relation between current density and the overall magnetic field it produces. This can be written as,

$$\vec{B} = \frac{\mu_0}{4\pi} \int \frac{\vec{J}(\vec{r}') \times \hat{r}}{r^2} d\tau', \quad (2)$$

which is Biot-Savart's law in its most common form. In principle the magnetic field inside the coils could be solved for at this point, but it is very inconvenient experimentally to find the current density and the distances for the \vec{r} vector.

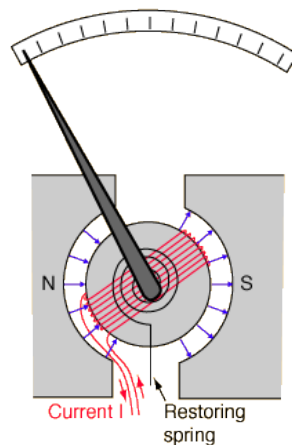


Figure 2. A Weston galvanometer with a current passing through the coils creating a torque in the magnetic field. This is opposed by the restoring spring.

From here we can derive a more experimentally friendly expression also known as Ampere's law. We begin by taking the curl of both sides of expression (2). This yields,

$$\vec{\nabla} \times \vec{\mathbf{B}} = \frac{\mu_0}{4\pi} \int \vec{\nabla} \times \frac{\vec{\mathbf{J}}(\vec{\mathbf{r}}') \times \hat{\mathbf{r}}}{r^2} d\tau'. \quad (3)$$

Then using the vector identity,

$$\vec{\nabla} \times (\vec{\mathbf{A}} \times \vec{\mathbf{B}}) = (\vec{\mathbf{B}} \cdot \vec{\nabla})\vec{\mathbf{A}} - (\vec{\mathbf{A}} \cdot \vec{\nabla})\vec{\mathbf{B}} + \vec{\mathbf{A}}(\vec{\nabla} \cdot \vec{\mathbf{B}}) - \vec{\mathbf{B}}(\vec{\nabla} \cdot \vec{\mathbf{A}}), \quad (4)$$

on the quantity inside the integral and considering only non-zero terms, the integral can eventually be simplified [4]. After using integration by parts and the vector identity, the right hand side of the expression in (3) can be rewritten as,

$$\vec{\nabla} \times \vec{\mathbf{B}} = \int \vec{\mathbf{J}}(\vec{\mathbf{r}}') 4\pi\delta^{(3)}(\vec{\mathbf{r}})d\tau' = \mu_0\vec{\mathbf{J}}(\vec{\mathbf{r}}), \quad (5)$$

where $\delta^{(3)}(\vec{\mathbf{r}})$ is the three dimensional Dirac delta function due to $\vec{\nabla} \cdot \frac{\hat{\mathbf{r}}}{r^2}$ [4]. This expression is just Ampere's law in differential form. Using Stoke's integral theorem Ampere's law can be written in terms of integrals instead of differential operators. Applying Stoke's theorem equation (5) becomes,

$$\iint (\vec{\nabla} \times \vec{\mathbf{B}}) \cdot d\vec{\mathbf{a}} = \iint \mu_0 \vec{\mathbf{J}} \cdot d\vec{\mathbf{a}}, \quad (6)$$

where the left hand side of the equation can be expressed as a closed integral as such,

$$\oint \vec{\mathbf{B}} \cdot d\vec{\mathbf{l}} = \iint \mu_0 \vec{\mathbf{J}} \cdot d\vec{\mathbf{a}} = \mu_0 I_{enc}. \quad (7)$$

Now we finally have the tools to treat the coils of wire in the Weston galvanometer. We can now exploit the contour integral on the left hand side of expression (7) to arrive at a simple expression for the magnetic field through the coils.

Because of the contour integral, we can use a closed Amperian loop to calculate the amount of magnetic field passing through the center of the coils. Looking at the cross section of the coils, as seen in Figure 3, we see that we have current travelling into the page as well as out of the page.

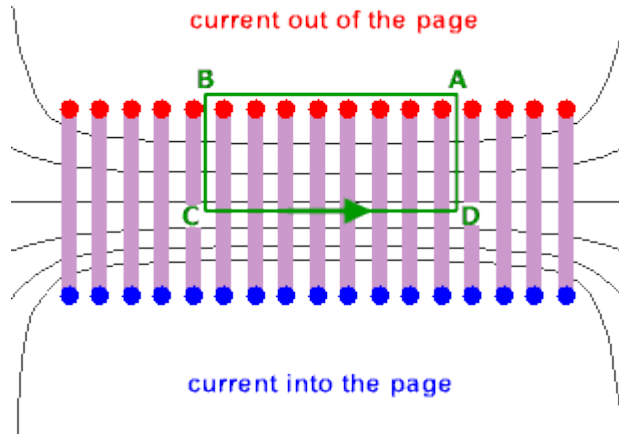


Figure 3. The cross section of the coils in a Weston galvanometer with the associated Amperian loop. The only component that contributes to the magnetic field is the line segment CD.

We can let the segment AB extent out to infinity such that the amount of magnetic field passing along that line is negligible. Also, the magnetic field along segments BC and DA are identically zero because the contributions from adjacent coils cancel as can be seen by the right hand rule. This means that the only segment that contributes to the magnetic field is the line CD. Equation (7) is then reduced to,

$$\oint \vec{B} \cdot d\vec{l} = \int_C^D \vec{B} \cdot d\vec{l} = Bl = \mu_0 NI, \quad (8)$$

where I is the current in the loop and N is the number of turns in the coil. The magnetic field produced by a current flowing in the coils can then be expressed in terms of the turn density, $n = N/l$. Finally, equation (8) can be rewritten as,

$$B = \mu_0 nI. \quad (9)$$

This is the magnetic field for a solenoid with current I and turns density n . When a magnetic moment such as this is created in an external magnetic field it will be subject to a torque as the magnetic moment tries to align with the external field. This torque can be expressed as,

$$\tau = M \times B, \quad (10)$$

where M is the magnetic moment or magnetization vector of the coils [4]. For a solenoid the magnetic dipole moment can be expressed as $M = NIA$, where A is the area of the circular coils. By placing the coils and needle orthogonally to the external magnetic field we can simplify the cross product so that the torque now reads,

$$\tau = NIAB. \quad (11)$$

All that is left to do is set the torque equal to the restoring force of the spring and solve for I . The resulting expression gives the current as a function of displacement and from there it is then possible to calibrate the galvanometer and use it as an ammeter. Also, solving for displacement as a function of current will allow the user to control the position of the needle or mirror with a signal. These two equations can be expressed as,

$$I = \frac{k\Delta x}{NAB} \quad \text{or} \quad \Delta x = \frac{Ik}{NAB}, \quad (12)$$

where k is the spring constant.

In this experiment it is the second equation of (12) that is important to us because the galvanometer mirrors must be controlled in order to produce a desirable image. In order to predict how a beam will behave when incident on one of the galvanometer mirrors it is important to examine a bit of light propagation and optics. The relevant principles here are Huygens' principle and the law of reflection.

Huygens' principle states that every point to which a luminous wave reaches becomes a source of a spherical wave and that the sum of the secondary waves determines the form of the main wave [5]. This principle can be applied to light waves incident on an interface and can describe the phenomena of reflection and refraction. In our case, light is incident upon the surface of a galvanometer mirror. When each part of the beam strikes the mirror it forms a spherical wave point source with the superposition of all the point sources forming the reflected ray. From Huygens' principle we can then find the law of reflection.

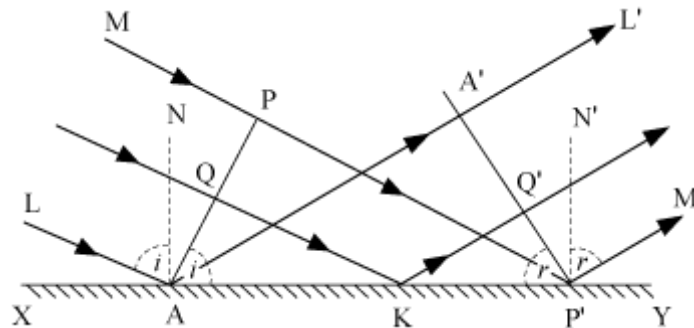


Figure 4. The geometrical construction of the law of reflection. It can be shown that $AA' = PP'$ and therefore $i = r$ [5].

Because the lower light ray strikes the mirrored surface before the upper ray does, in Figure 4, the spherical wave point source at A begins propagating light before the point sources at K or P' will and therefore will force plane waves to travel to the right. When the light strikes at point A it is only at point P for the upper ray. Therefore as the light travels from point P to P', light will also propagate from point A to A' the same amount of time and form a plane wave line segment A'P'. Because light rays travel at the same velocity, line segments AA' and PP' are equal. If we form two triangles AP'A' and AP'P that share AP' and have equal sides AA' and PP' we can conclude that they are similar triangles and therefore have the same angles i and r . Therefore we have proved the law of reflection.

This tells us how the beam behaves as angle of incidence changes, but in this case it is the galvanometers that will change pitch relative to the beam. That simply means that as the galvanometers change an angle θ , the beam will be reflected through an angle 2θ [5]. Because the experimental system has two perpendicular mirrors that rotate in orthogonal directions, each mirror will be able to control the beam movements in the horizontal and vertical axes of the target plane independently [6].

System overview

An overhead view of the experimental system is shown in Figure 5. A Nutfield QuantumDrive-1500 model mirror mounted galvanometer system was connected to a $\pm 20V$ supply with signal inputs wired to LabJack U12 analog output ports which were controlled by homemade LabView (National Instruments) code. It is also important to note that at points in the bandwidth measurements the signal inputs were instead wired to an Agilent 33220A function generator. A 5 mW, 532 nm diode laser powered by a +3V supply was used as the Gaussian beam because of the intensity of its output radiation. The ensemble was mounted to an aluminum slab with additional banana jacks to increase the systems modularity and to make it more robust as the individual components are quite fragile.

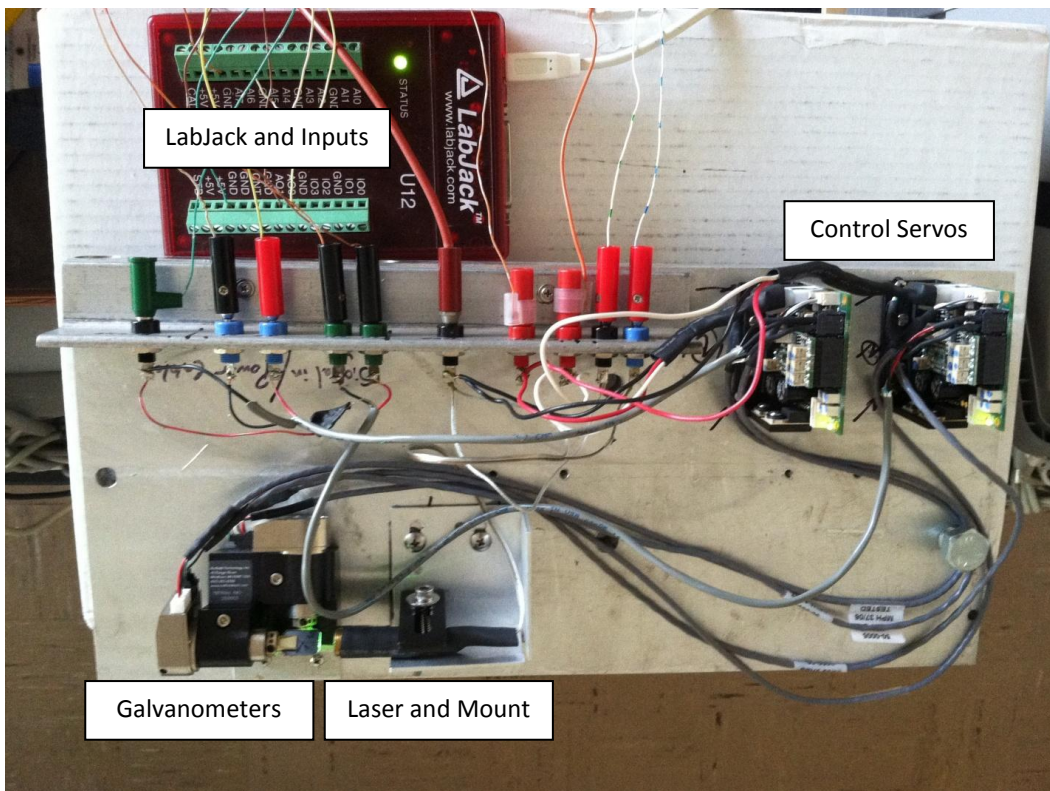


Figure 5. Overhead view of the experimental apparatus with Nutfield galvanometers, laser and mount, control servos, and LabJack connections. Here everything has already been mounted on the aluminum plate. Not pictured are the power supplies and the LabView software.

Connectors had to be made for both servo boards. This included input signal connections and power connections. Each connector and wire was shrink-wrapped together to ensure the integrity of the connections. Also leads were soldered onto the banana jacks to ensure good electrical contact and to improve the modularity of the ensemble. The power supplies were wired to have bipolar and unipolar configurations for the servo boards and the laser respectively.



Figure 6. The wiring configurations for a bipolar or unipolar power supply. The image on the left is +3V used to power the laser and on the right is $\pm 20V$ for the servo boards.

Homemade National Instruments LabView code was used to control and drive the servo board signals. This code, as seen in Figure 7, interfaces with the LabJack's Analog Output (AO) pins via the Easy Analog Output (EAO) function in order to provide a signal to the servo boards to control the position of the mirrors. The vertical servo board was connected to AO0 on the LabJack and the horizontal servo board was connected to the AO1 output.

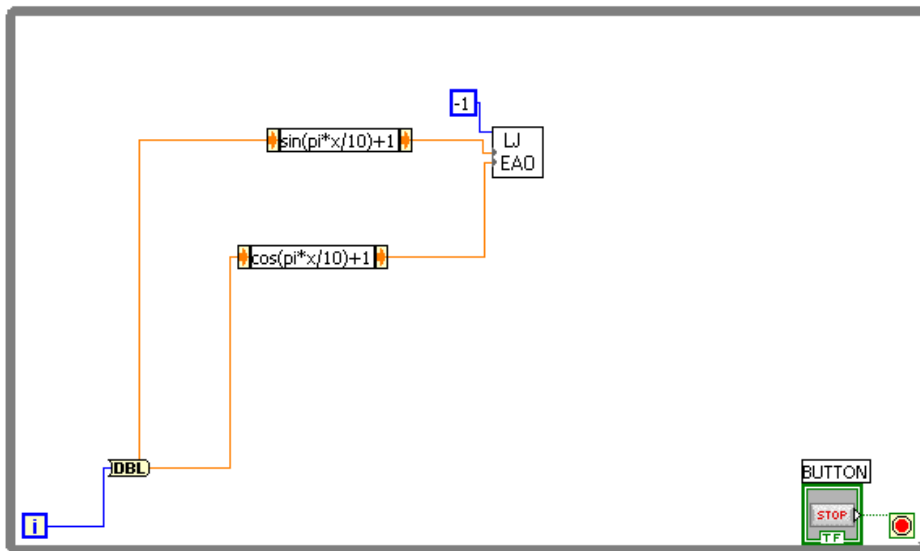


Figure 7. The custom National Instruments LabView code used in this experiment to control the galvanometer mirrors. The vertical axis is dictated by a sine function while the horizontal axis is dictated by a cosine function in order to produce a circular display.

In the LabView code, compensations are made in the sine and cosine functions to account for the 0-5V analog output parameters in the LabJack. Therefore, a DC offset must be applied to the waveforms to prevent them from dipping below 0V. In the argument, the frequency is controlled by the scalar multipliers (in units of radians) applied to the variable x , which is tied to the iterations of the while loop. This fact serves as the limiting factor to this experiment because it puts a cap on the maximum resolution of the waveform we can obtain, thus deforming the output waveform at higher frequencies.

The code in Figure 7 produces a circular figure, as can be seen in Figure 11, on the target plane which was used to test the system's ability to function as a laser light display. To measure the frequency response and the mirror displacement per volt, the code was modified to only output to one pin on the LabJack at a time. The amplitude and frequency of the waveforms could then be changed depending on the data needed.

Analysis of data

Since the LabJack could only output an analog signal between 0-5V, the maximum mirror displacement for the sake of bandwidth measurements was taken with a waveform that oscillated from 0-5V. The frequency was then incremented from 1 to 250 Hz with the mirror displacement recorded.

In order to drive the mirrors at the desired frequency the correct scalars in the sine and cosine arguments needed to be determined. Using the clock function in LabView it was determined that the while loop went through 62.48 iterations per second. This is the rate at which the variable x proceeds through the various values of the sine function. Since we needed the frequency it was sufficient to find the time it took for the program to complete one period of sine. Using the form $A \sin(\pi x/b)$ with $x = 62.48$ loops/s and b an arbitrary constant of our choosing,

$$\frac{\pi x t}{b} = \frac{62.48 \pi t}{b} = 2\pi, \quad (13)$$

gives us the an expression for the amount of time t it takes to process one period or 2π . Solving for t ,

$$t = \frac{2b}{62.48} = 0.032b \rightarrow f = \frac{1}{t} = \frac{31.24}{b}, \quad (14)$$

leads to the frequency of the waveform if we substitute for b into the LabView code. We can now create a waveform of arbitrary frequency to drive the mirrors.

Mirror Displacement (cm)	Mirror Frequency (Hz)	b constant
57.1	1	31.24
56.8	3.124	10
55.9	10	3.124
52.6	50	0.625
47.8	100	0.3124
0	250	0.125

Table 1. The measured maximum mirror displacement in cm at each calculated frequency with corresponding b.

The frequencies at which the mirrors were driven are given in Table 1. A very wide range of frequencies was initially chosen ranging from 1 Hz to 1 MHz, but we stopped at 250 Hz because it failed to produce any pattern. This result was pretty standard considering the mechanical nature of the galvanometers and the forces necessary to rotate the mirrors at considerable speeds.

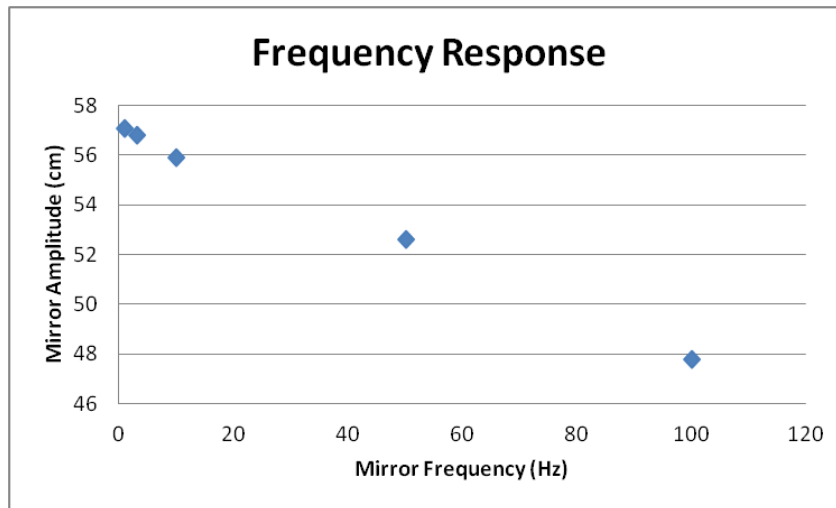


Figure 8. Plot of maximum mirror amplitude in cm versus mirror frequency to calculate bandwidth. The 3dB point is usually used to measure bandwidth, but we had to use other methods.

As seen in Figure 8, the mirror amplitude abruptly stops because there was no system response to the 250 Hz signal. This makes measuring the bandwidth an interesting affair. Usually the bandwidth is taken when the signal drops below the 3 dB point, but our data drops off abruptly making it difficult to determine.

In order to confirm that the system responds poorly to signals around 250 Hz, the LabJack signal input was changed for an Agilent 33220A function generator. The frequency was ramped up quickly to 250 Hz where the frequency was then incremented one Hz at a time until the output pattern ceased to be desirable. This happened at 275 Hz where the pattern began to

exhibit hysteresis on not just the horizontal axis where the measurements were made, but the vertical axis as well. It is also interesting to note that this is when the status LEDs on the servo boards lit up red signifying some kind of error or overload. Also, as the frequency was being increased, noticeable shortening of the pattern began to occur at 175 Hz. Regardless of the shortening the pattern exhibited no hysteresis and still responded well enough at that frequency to still be an adequate laser display. In light of these findings, the operational bandwidth of this device is being reported at 250 Hz in order to limit the risk of damage to the electronics.

The next task at hand is to determine the sensitivity of the mirrors by calculating the angle of rotation per volt of signal. To do this we consider the triangle formed by the laser when the signal is applied and, using trigonometry, calculate the angle swept out at each signal voltage.

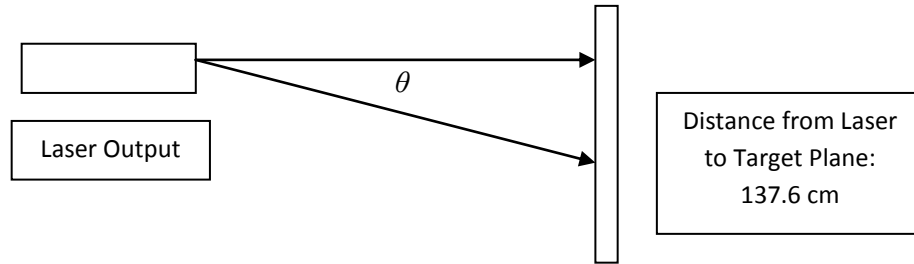


Figure 9. Experimental schematic of degree/volt measurements. Distance to target plan is 137.6 cm.

Because the distance to the target plan is known along with the distance the beam is swept out, we can calculate the corresponding angle of the right triangle using the inverse tangent function. The distance to the target plane is the horizontal component of the triangle while the distance swept out is the vertical component. This gives and expression for the angle,

$$\tan(\theta) = \frac{\text{distance swept out}}{\text{distance to target}}, \quad (14)$$

which yields,

$$\theta = \tan^{-1} \left(\frac{\text{distance swept out}}{\text{distance to target}} \right). \quad (15)$$

Using equation (15), the angular displacement of the mirrors was found for different signal voltages. All of the signal voltages were at 3.124 Hz which was well within the bandwidth limitations for the apparatus. This ensures that all of the angles will be accurate angles and not reduced by mechanical or electronic breakdowns in the system.

Signal Voltage (V)	Display Amplitude (cm)	Angular Displacement (degrees)
5	57.5	22.7
4	45.3	18.2
3	33.6	13.7
2	22.1	9.1
1	11.1	4.6

Table 2. For each signal voltage the corresponding mirror displacement was found. Using trigonometry the angular displacement was calculated.

It is important to note again that the signal only oscillates between 0 and a voltage +V because of the output parameters of the LabJack. If the waveform had no DC component and was centered around 0V, the mirrors would sweep out an angular displacement in the negative (opposite) direction as well.

From Table 2, we see that the maximum angular displacement was found to be 22.7 degrees. This value was found to support the manufacturer's specification of 20.0 degrees with a difference of 13.4%. From the plot of the data in Figure 10, we can conclude that the angle of rotation per volt is just the slope of the line of best fit. This was calculated to be 4.55 degrees of rotation per volt. This compared favorably to the data provided by the specifications sheet which put the rotation at 4 degrees per volt, a different of only 13.8%. For a private laser light display this number is more than adequate considering the target area will be fairly small compared to the possible distances we can place between the apparatus and the screen.

In order to fully determine the system's ability to adequately function as a laser light display a circular pattern was displayed on the target plane for observation while frequency and amplitude in the horizontal and vertical directions was changed.

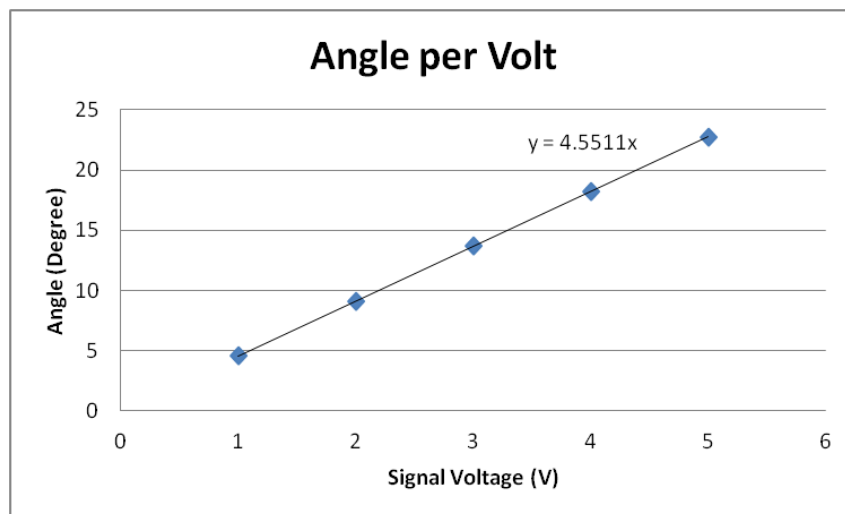


Figure 10. Plot of mirror displacement in degrees versus signal voltage. Here the slope of the graph determines the angular displacement per volt of signal.

First the pattern was created at a frequency of 3.124 Hz as depicted in Figure 6. As seen in Figure 11, the circle is seen traced out by the diode laser at such a speed so that an observer cannot see a full circle on the target plane. In an attempt to fool the observer's eyes and view a solid circle on the target plane the frequency of oscillation was increased. This, however, had unforeseen consequences.

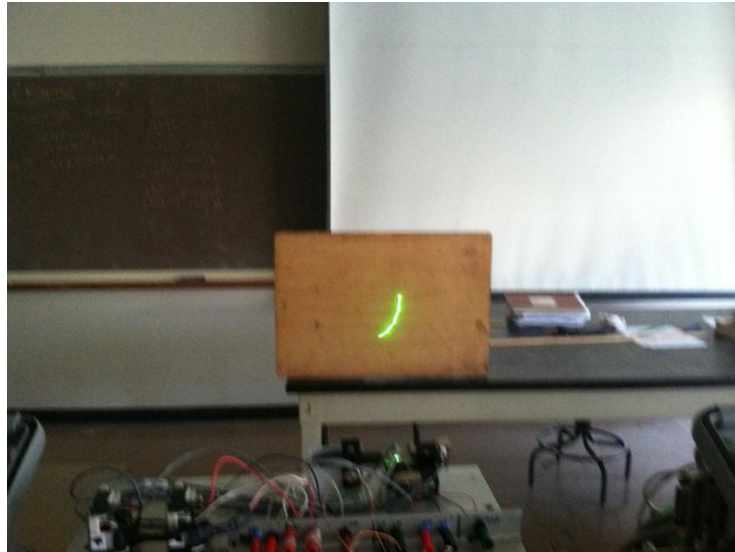


Figure 11. A circular pattern was displayed on the target plane with an overall frequency of 3.124 Hz.

As the frequency was incremented, the data points on the sine and cosine waves in the LabView code became more dispersed in space and time leading to less circular paths. At high enough frequencies (on the order of 10-50 Hz) the circle ceased being a circle as the data points jumped over large arc lengths and became chords rather than arcs. This produced some very fascinating and interesting, but ultimately unwanted and unacceptable images on the target plane.

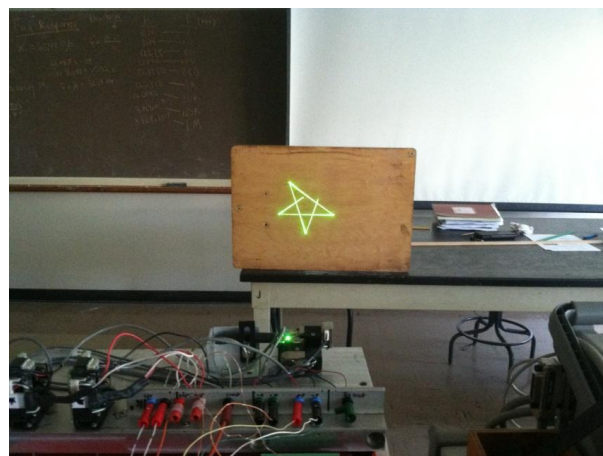


Figure 12. The trace of a circle at around 50 Hz results in the image of a spinning star—an interesting but unwanted pattern.

At around 30 Hz the circle no longer looked like a point tracing out the image of a circle, as desired, but no longer retained the shape of a circle, rather, it held the shape of a triangle. Increasing the frequency to 50 Hz resulted in a star-shaped pattern than slowly rotated counter-clockwise. This pattern would be very difficult to make using sine and cosine parametric equations, so it is potentially an advantage for the system to behave this way. Albeit, it is not an advantage if it comes at the expense of the ability to make arbitrary circular shapes. Sadly, this attribute of LabView, and thusly the system as a whole, greatly lowers the potential of it being used as a laser light display capable of making complex shapes. As of right now the apparatus is limited to tracing out shapes of different plots produced using parametric equations.

Discussion

During the course of the experiment several inefficiencies were found in the system. Using solely the LabJack as an analog signal output proved to be problematic and did not give us access to the full range of motion available to the galvanometers. The LabJack analog outputs are designed and configured to only output a signal in the range of 0-5V, but the servo boards and the galvanometers are designed to accept $\pm 5V$. This means that we were only operating in the positive regime for both horizontal and vertical axes. This effectively limited us to one quadrant of the full range of motion for the system. To keep the signal within this quadrant a DC offset had to be applied to the signal waveform thereby further decreasing the signal amplitude and the amount of displace we could achieve in any one direction. This is not the largest limitation of the system as it only affects the size of the image and not necessarily its quality.

To further complicate the issue we were limited to a certain amount of data points per second to build the desired waveform. This resolution limit was determined by how fast the computer and the LabView software could iterate the main while loop as seen in Figure 6. This was discovered to be 62.48 loops/s. At lower frequencies, 62.48 data points per second is more than enough to produce a smooth waveform and therefore a continuous display, but it is not fast enough for the eye to perceive the trace as one image. At higher frequencies the data points become more spread out over the waveform because more of the sine wave needs to be constructed per unit time. This causes the waveform to lose continuity as it appears to be made up of multiple line segments rather than a continuum of points. At this point the output image is adversely affected as sections of arcs become straight line segments causing the circular output to look like a triangle or a rotating star. This was the biggest limitation to the system that we discovered.

To remedy these two issues, several solutions were proposed. Adding external circuitry between the LabJack outputs and the servo boards is one possible solution to gain access to the full range of motion. This would require removing the DC component of the signal and then amplifying the signal with either an operation amplifier or a transistor amplifier. This would make the displays larger, and, as a result, would also make the resolution issue at higher frequencies more pronounced. It would also force the mirrors to sweep across a larger area in the same amount of time increasing their angular velocity and potentially shortening the bandwidth.

Another proposed solution involved replacing the LabView-powered LabJack output with the Agilent 33220A function generators used in the frequency response measurements. The function generators would preferably be controlled by a C program in a UNIX environment where speed and loop iteration rate would not become limiting factors. Here a signal of $\pm 5V$ could be created without any external circuitry and a much higher sampling rate could be

achieved such that no deformation of an output image would be apparent. The drawback of such a system is the need for two function generators and their availability in the place the system is currently operated. Nonetheless, the advantages the function generators and a C program can provide over the current LabView/LabJack system far outweigh the slight modularity loss of having to provide two function generators at the location of operation.

Conclusions

We have constructed a laser light display using Nutfield QuantumDrive-1500 model mirror mounted galvanometers. We investigated the frequency response, angle per volt, maximum angle, and the system's ability to function as a laser display using a circular pattern. The bandwidth was found to be 250 Hz when the galvanometers began to cease functioning, while the angle per volt was found to be 4.55 degrees per volt with a 22.7 degree maximum scanning angle in one direction. The degree per volt measurements were found to agree with the manufacturer's specification of 4.0 degrees per volt with a difference of 13.8%. The maximum scanning angle measurements were also in close agreement with the specifications. The manufacturer reported the maximum scanning angle to be 20.0 degrees, which corresponds to a difference of 13.4%. It was also discovered that the output display could only have a maximum of 62.48 data points per second. We found that this value in particular played the most important role in the performance of the system.

This value hampered bandwidth measurements, which also had an effect on the rotation measurements, but had the most profound effect on the system's ability to perform as a laser display. At frequencies around 50 Hz and higher the output image was severely distorted as arc segments could no longer be displayed.

Several potential upgrades to this system were discussed earlier, but the most dramatic and complete change to this system involve omitting the LabJack signal output completely and replace it with a C program in a UNIX environment and two Agilent 33220A function generators as used in some of the bandwidth measurements. This would eliminate mirror displacement issues as well as resolution issues at all frequencies allowing the system to function adequately as a laser light display.

In this experiment the construction of a laser light display and the analysis of some of its core features was undertaken. The frequency response, angle of mirror rotation per volt, and maximum angle of mirror rotation were found and reported. The system was found to behave poorly as a laser light display in its current state, but future upgrades have been discussed and are intended to be implemented. As the first steps to constructing a laser light display at Cal Poly, we believe this study to be a success.

References

- [1] R.D.L. Hanes, M.C. Jenkins, S.U. Egelhaaf, "Combined holographic-mechanical optical tweezers: Construction, optimisation and calibration," American Institute of Physics: Review of Scientific Instruments, **80** (2009).
- [2] S.Engel, et al., "Folding and unfolding of a triple-branch DNA molecule with four conformational states," Philosophical Magazine, **91**, 2049-2065 (2011).

[3] D. Hover, et al., “Superconducting Low-Inductance Undulatory Galvanometer Microwave Amplifier,” *Journal of Applied Physics*, **110** (2011).

[4] D.J. Griffiths, “Magnetostatics,” in *Introduction to Electrodynamics Third Edition*, A.Reeves and K. Deltas, eds. (Prentice-Hall, 1999), 202-232.

[5] P. Mouroulis and J. Macdonald, “Rays and the Foundations of Geometrical Optics,” in *Geometrical Optics and Optical Design*, M. Lapp, et al., eds. (Oxford University Press, 1997), 3-15.

[6] F. L. Pedrotti, et al., “Geometrical Optics,” in *Introduction to Optics 3rd Edition*, E. Fahlgren, et al., eds. (Pearson Education, 2007), 16-42.